International Journal of Environmental Science and Technology
https://doi.org/10.1007/s13762-021-03313-2

ORIGINAL PAPER

Biosorption of hexavalent chromium and Congo red dye onto *Pleurotus mutilus* biomass in aqueous solutions

A. Alouache[1] · A. Selatnia[2] · H. E. Sayah[3] · M. Khodja[4] · S. Moussous[5] · N. Daoud[2]

Received: 24 July 2020 / Revised: 7 March 2021 / Accepted: 8 April 2021

Abstract

With the significantly increasing pharmaceutical and antibiotics industry in Algeria, the elimination of biomass is of utmost importance since the latter represents a large part of waste from the manufacturing process. In this work, the elimination of hexavalent chromium Cr (VI) and Congo red dye is part of the *Pleurotus mutilus* biomass recovery process. Thus, biosorption has been studied in a discontinuous system. Optimal conditions were estimated by variations in contact time, temperature, initial pollutant concentrations, and simultaneous removal of both pollutants. The greatest uptake capacities achieved were 36.68 mg/g of and 15.08 mg/g of Cr(VI). The initial concentrations of both pollutants being equal to 50 mg/l, for a duration time of 180 min and a temperature of 300 K. Based on the values of the coefficient of determination R^2, χ^2, and ARE, the isothermal equilibrium data were better represented by Freundlich, Temkin, and Dubinin-Radushkevich models. The kinetic biosorption of the two pollutants was well described using the pseudo-first-order model. The biosorption process is controlled by external mass transfer. The physical process in nature of Cr(VI) and (CR) biosorption has been justified based on the values obtained of $\Delta G°$ and $\Delta H°$. Globally, this work demonstrates the considerable potential of *Pleurotus mutilus* for the elimination of anionic pollutants. Research results indicate that this biomass, a waste material, first destined for incineration, was recovered without any treatment. Due to its low cost, it could serve as an inexpensive source for recovering heavy metals and dyes from dilute contaminated water.

Keywords Congo red · Hexavalent chromium · *Pleurotus mutilus* · Biosorption · Kinetics · Wastewater

Abbreviations

q_t	The instantaneous uptake capacity (mg/g)
q_e	Equilibrium uptake capacity (mg/g).
K_1	Constant of first-order rate (min^{-1}).
K_2	Pseudo-second–order constant (g/(mg.min))
K_i	The diffusion rate constant ($mg/(g.min^{0.5})$)
$t^{0.5}$	Time square root of time ($min^{0.5}$)
F	The ratio of the instantaneous to the equilibrium solute adsorbed
B_t	A function depending on F
q_m	The maximum uptake (mg/g)
b	The equilibrium Langmuir constant (L/mg)
R_L	Langmuir distribution factor
C_t	The solute concentration at time t (mg/L)
C_e	The concentration at equilibrium (mg/L)
C_0	The concentration at the initial time (mg/L)
m	Biosorbent weight (g)
V	Volume solution (L)
K_F	Constant of Freundlich isotherm
K_T	The Temkin binding constant at equilibrium (L/g)
T	Temperature (K)
B	Temkin constant depending on the heat of biosorption (J/mol)
R	The universal gas constant

Editorial Responsibility: Samareh Mirkia.

✉ A. Alouache
ali.alouache@g.ens-kouba.dz

[1] Laboratoire de Biologie Des Systèmes Microbiens (LBSM), Ecole Normale Supérieure, B.P. 92, 16050 Kouba, Alger, Algeria

[2] Départements de Génie Chimique, Ecole Nationale Polytechnique, 10 Avenue Hassen Badi, BP 182, 16000 El Harrach, Algeria

[3] Université M'hamed Bougara de Boumerdes, Avenue de l'indépendance, 35000 Boumerdes, Algeria

[4] Sonatrach /Institut Algérien du Pétrole, Avenue du 1er novembre, 35000 Boumerdès, Algeria

[5] Ecole Militaire Polytechnique (E.M.P), Bordj El-Bahri, Alger, Algeria

Published online: 23 April 2021

β	Activity coefficient in the Dubinin-Radushkevich model (mol^2/J^2)
E	Average free energy of biosorption
ε	Polanyi potential (kJ/mol)
$\Delta S°$	Entropy variation (kJ/mol.K)
$\Delta G°$	The free enthalpy variation (kJ/mol)
$\Delta H°$	The enthalpy variation (kJ/mol)
K_L	The equilibrium constant equal q_e/C_e

Introduction

Contamination of water sources with synthetic dyes and heavy metals from many industries has created major environmental threats. Many of these dyes, namely Congo red (CR), are toxic and even carcinogenic. The total dye production in the world is around 700 000 tons per year, 10% of which are lost in the effluents during the various stages of application and preparation (Bouras et al. 2017; Dawood and Sen 2012).

Azo dyes are largely used compared to many synthetic dyes. This type of dye reaches 70% of industrial colorants consumed annually (Schmidt et al. 2019). The Congo red which is classified in this category and used in many industries known as a popular anionic dye can be converted into benzidine which makes it carcinogenic (Zhang et al. 2011). Several studies have reported the toxicity of dyes in wastewater according to (Bouras et al. 2017; Dawood and Sen 2012; Panda et al. 2009). Effluents contaminated with dyes affect the ecosystem and aquatic health and inhibit sunlight penetration (Panda et al. 2009). They can affect plant life, as well as destroy flora and endanger natural ecosystems (Bouras et al. 2017). The increase in the concentration of dyes in the environment is very harmful due to mutagenic, genotoxic, and teratogenic effects on living organisms (Schmidt et al. 2019). Approximately 10–15% of the used dyes discharged in the enclosed state into water plans cause skin irritation, dermatitis, cancer, kidney, liver, and reproductive system dysfunction in humans (Shaban et al. 2017). Besides, there are some processes employed to reduce the dye pollution such as biological treatment (Wanyonyi et al. 2019), membrane filtration (Nadeem et al. 2019), photodegradation (Zhu et al. 2019), biodegradation (Ortiz-Monsalve et al. 2017), catalytic ozonation (Ghuge and Saroha 2018), and electrochemical oxidation (Ramírez et al. 2016).

Heavy metals represent a colossal wastewater disposal problem. Among these heavy metals, hexavalent chromium Cr(VI) is widely used in metal finishing, paint, paper industries, electrical, and electronic equipments as well as catalysts in chemical manufacturing (Mohagheghian et al. 2017). The two main oxidation forms of chromium are trivalent and hexavalent. The latter being much more toxic causing environmental pollution, directly affecting public health (Kavitha et al. 2016). Hexavalent chromium can be considered responsible for several health hazards (Ghaneian et al. 2017). Human interventions are the main cause of elevated chromium levels in the aquatic environment, groundwater, and spring water (Dermatas et al. 2015; Khitous et al. 2016). It was noted by the International Agency for Research on Cancer that hexavalent chromium has been classified as a human carcinogen (Mohagheghian et al. 2017); it has a toxic effect even at diluted concentrations. The maximum allowable concentration for drinking water, as defined by (WHO) World Health Organization, is 0.05 mg/L (Fontana et al. 2016). However, the maximum limit for chromium content has been fixed to a value of 0.1 mg/L for drinking water according to the Environmental Protection Agency (Mohagheghian et al. 2017). Greater quantities of chromium are released to industrial wastewater, with concentrations up to 220 mg/L, contaminating soil and water. For this reason, many studies have recently focused on the elimination of heavy metals and dyes present in wastewater (Chang 2019). Consequently, traditional processes are used for the removal of chromium including electrochemical precipitation (Kongsricharoern and Polprasert 1996), ion exchange (Zhou et al. 2018), solvent extraction (Pagilla and Canter 1999), and chemical precipitation (Zhoui et al. 1993) or membrane separation (Hafiane et al. 2000).

In the processes of the complete elimination of many types of dyes and heavy metals (Foroughi et al. 2014), conventional biodegradation is ineffective (Afroze and Sen 2018). These processes have high operational costs especially in maintenance and energy requirements and become ineffective at low concentrations of metal ions and dye (Bouras et al. 2017; Dawood and Sen 2012). Currently, in terms of cost, biosorption can be considered as one of the most widely used and attractive processes (Bouras et al. 2017). Inexpensive and efficient biomaterials used in the purification of water, are an alternative for many environmental research programs (Foroughi et al. 2014; Gupta and Suhas 2009). Groups in the fungal cell wall of biomass can form bonds toward heavy metals and dye, making biosorption more favorable (Cherifi et al. 2014). Waste from the antibiotics industry generates different types of fungal material such as *Pleurotus mutilus* and *Streptomyces rimosus*. These materials are cheap, available, and abundant; for these reasons, they are used as biosorbents for the treatment of pollutants in wastewater, particularly dyes as well as heavy metals (Wu et al. 2018).

The overall objectives of the present study include the evaluation of the fungal biomass of *Pleurotus mutilus*, an industrial bioproduct available in large quantities, as a biosorbent for (CR) dye and Cr (VI) ions as target anionic pollutants in aqueous solutions.

Congo red dye and Cr (VI) both have significant impacts on the environment causing mutagenic and/or carcinogenic

effects as well as considerable damage to the ecosystem. They are resistant to biological degradation and quite difficult to eliminate.

In textile drainage, elevated levels of certain metals such as Cr (VI) are found along with dyes, as Cr metals are generally used as mordents (i.e., color fixing agents) (Kumari et al. 2018).

The research survey indicates that the simultaneous adsorption of hexavalent chromium and Congo red dye onto the *Pleurotus mutilus* biomass has not been yet investigated.

The characterization of this biomass and the influence of initial concentrations and initial pH were carried out. Thermodynamic, equilibrium, and kinetic models have been developed to assess the possibility, adsorption capacity, and the step controlling biosorption rate of Congo red and hexavalent chromium on the *Pleurotus mutilus* biomass. Competitive adsorption capacity was used to evaluate the CR and Cr(VI) adsorption performance in the binary mixture.

Materials and methods

Pleurotus mutilus biomass preparation

This biomass, which is a fungal waste, was generated as a residue of non-living *Pleurotus mutilus* filamentous fungi biomass, produced during veterinary antibiotic *Pleuromutiline* production. It was obtained from SAIDAL Antibiotical Complex (Medea, Algeria). Usually, this waste is destined for incineration; it can be recovered for wastewater treatment. This waste was washed three times using distilled water and after that dried at 60 °C for 24 h. Finally, this biomass was manually crushed and sieved before being stored for adsorption experiments.

Pleurotus mutilus biomass characterization

It is necessary to determine adsorbent's physicochemical properties for their use in wastewater. The determination of characterization parameters helps to explain the phenomena that govern the capacity and efficiency of adsorption.

Determination of zero point charge

The zero charge point is defined as the pH where the number of positively charged centers is equal to the number of negatively charged centers that correspond to a zero charge on the outer surface of a particle. The determination of the zero charge pH point (pHzpc) was performed by adding 0.1 g of biomass to 50 ml of 0.01 M KNO_3 solution (1.01 g/L) whose initial pH was measured and adjusted with 0.1 M HCl or 0.1 M NaOH solutions. The container was sealed and placed on a stirrer for 48 h at room temperature before measuring the pH of the solution. The zero charge point (pHzpc) is the value at which the curve $pH_{initial}$ $pH_{final} = f(pH_{initial})$ intersects the $pH_{initial}$ axis (Blanes et al. 2016).

FTIR spectroscopy

Spectroscopy is an important technique used to identify the functional groups characteristic of the surface of the adsorbent. These groups are often responsible for the adsorbent–adsorbate bonds.

The absorption phenomenon in the infrared domain is linked to molecular vibration phenomena, which implies a variation of the dipole moment and therefore the creation of a magnetic field. Each group vibration gives rise to an absorption band corresponding to a certain intensity which generally varies from one group to another and which is used for the qualitative analysis of the functional groups present on the surface of the biomass.

Infrared spectra of powdered *Pleurotus mutilus* were obtained after drying the biosorbent mass at 343 K for 24 h. The principle of the analysis consists of recording the vibrations of the functional groups between 200 and 4000 cm^{-1} using a SHIMADZU spectrophotometer model FTIR-8400 by mixing a finely powdered sample with potassium bromide (1:10). The characteristic functional groups at the adsorbent surface, which are frequently responsible for adsorbant–adsorbate bonds, were identified by spectroscopy which is considered as an important technique (Zbair et al. 2018).

Boehm titration

Acid and base sites on the biosorbent were determined using the acid–base titration method proposed by (Boehm 1994). Samples of 0.5 g of biomass in triplicate were stirred with 50 ml solution of $NaHCO_3$ (0.1 M), Na_2CO_3 (0.05 M) and NaOH (0.1 M) for the acid groups and 0.1 M HCl for the basic groups, respectively, at room temperature (24 ± 2 °C) for 72 h in closed centrifuge tubes. The stock solution was prepared from an analytical grade product (Merck, Darmstadt, Germany) in deionized water. The equilibrium Boehm reagents were separated from the biomass by filtration (Fidel et al. 2013). The isolated solution underwent acidification followed by boiling to remove CO_2. To determine the quantity of the equilibrium Boehm reagents that were neutralized during the initial equilibrium Boehm equilibrium with the solid, aliquots of the isolated solutions are titrated back with a standardized solution of NaOH (Fidel et al. 2013).

Scanning electron microscopy

The surface characteristics of the Pleurotus mutilus biomass were examined by scanning electron microscopy (Zeiss EVO 40 EP microscope).

Thermogravimetric and X-ray fluorescence analyses.

A NETZSCH TG 209F3 Thermogravimetric Analyzer was used to perform a thermogravimetric examination of the biosorbent particles. Samples of 5 mg were analyzed from 26 to 350 °C under an inert atmosphere (nitrogen flow 20 ml/min) to avoid side reactions such as oxidation. The spectrometer used for μXRF is A Shimadzu RF-1501 XRF; it has a rhodium X-ray source.

The mineral residue quantitative elemental analyses resulting from TGA were carried out under the following operating conditions: a voltage of 30 kV, a current of 0.02 to 1.00 mA (with a minimum increment of 0.02 mA).

Congo red dye and hexavalent chromium preparation

Congo red dye (CR) and hexavalent chromium have been used in this study as target pollutants to estimate the removal capacity of *Pleurotus mutilus* biomass. Stock solutions of the two synthetic pollutants have been prepared by adding the appropriate quantities of powdered dye and potassium dichromate to distilled water. For all experiments, successive dilutions were made to have different concentrations. In Fig. 1 it can be seen the developed molecular structure for Congo red (Chauhan et al. 2017).

Batch experiments

Erlenmeyer flasks containing biomass and 100 ml of biosorbent solution were used to perform experiments. The stirring speed has been fixed at 250 rpm. Samples were taken in predefined periods; biosorbent recovery for (CR) was done using centrifugation (EZ Swing 3 k) at 12,000 rpm. Liquid solutions were analyzed using an ultraviolet UV–Visible spectrophotometer (OPTIZEN 1412 V) at wavelengths of 500 nm.

$$q_t = \frac{(C_0 - C_t)V}{m} \tag{1}$$

For the chromium analysis, sampling was followed by filtration to remove the biomass from the solution. The residual chromium concentration was determined by adding 1,5-diphenylcarbazide (DPC) to the liquid phase and analyzing it at 540 nm under acidic conditions (Ajmani et al. 2019; Chatterjee et al. 2019). The uptake capacities of Cr(VI) ions and (CR) dye have been obtained by the equation as follows:

Several solutions containing 100 mg of *Pleurotus mutilus* biomass were prepared by changing the initial concentrations for (CR) dye and Cr(VI) ions. At equilibrium, the uptake capacities can be expressed using Eq. (2).

$$q_e = \frac{(C_0 - C_e)V}{m} \tag{2}$$

A binary adsorption assay was performed with a total concentration of 100 ppm in aqueous solutions at different ratios of Cr (VI) and (CR). In order to investigate their simultaneous elimination, biomass (0.1 g) was added to 250 ml of Erlenmeyer flasks containing a mixture of (CR) and Cr (VI) in 200 ml of an aqueous solution. The flasks were stirred at room temperature at 250 rpm. The solutions used were prepared accordingly: solution 1 (30% (CR) and 70% Cr(VI)), solution 2 (50% (CR) and 50% Cr(VI)), solution 3 (70% (CR) and 30% Cr(VI)).

To identify the adsorption behavior of Cr(VI) and (CR) in the binary mixture, the competitive adsorption capacity was used. Adsorption was carried out close to optimum adsorption conditions at a fixed pH and contact time. Equation (3) is used for estimating the percentage of removal of the Cr(VI) ions or (CR) dye attached to the biomass.

$$R\% = \frac{C_0 - C_e}{C_0} \times 100 \tag{3}$$

To assess the adequacy of the isothermal equations, the Chi-square (χ^2) and mean relative errors (ARE) were calculated from the following equations (Rasool and Lee 2013):

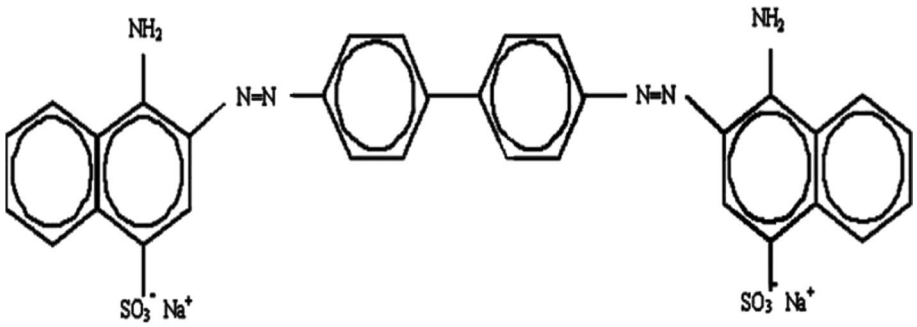

Fig. 1 Congo red molecular structure

$$\chi^2 = \sum \frac{\left(q_{e,\mathrm{calc}} - q_{e,\mathrm{exp}}\right)^2}{q_{e,\mathrm{exp}}} \quad (4)$$

$$\mathrm{ARE} = \frac{100}{n} \sum_{i=1}^{n} \left| \frac{q_{e,\mathrm{calc}} - q_{e,\mathrm{exp}}}{q_{e,\mathrm{exp}}} \right| \quad (5)$$

where n is the number of experimental data points, $q_{\mathrm{e,\ exp}}$ is the measured ion concentration, and $q_{\mathrm{e,\ calc}}$ is the calculated ion concentration with models.

Results and discussion

Characteristics of *Pleurotus mutilus* biomass

The point of zero charge (pHzpc)

The pH value of the solution, where the surface charge density is zero, corresponds to the zero charge point (pHzpc). If the pH is inferior to pHzpc, the surface of the sorbent becomes positively charged. If the pH is higher than pHzpc, a negative charge will be applied to the surface of the biosorbent. The pHzpc (zero charge point) is defined as the value at which the curve pHinitial pHfinal = f (pHinitial) intersects the pHinitial axis (Blanes et al. 2016) (figure not shown here). The pHzpc value obtained was 7.94. Therefore, at a pH value below 7.94, the surface of the *Pleurotus mutilus* biomass is positively charged. For this pH value, the negatively charged species such as Cr(VI) ions and the (CR) dye are strongly attracted to the biomass.

Infrared spectra

The results of the physical and chemical analysis of this biomass were enhanced by FTIR spectroscopy. The infrared spectroscopic analyses of *Pleurotus mutilus* are shown in Fig. 2. The most intense bands and their corresponding groups existing on the biomass surface are explained as follows:

- The groups (–OH) or (–NH) match the first vibration recorded at 3438.23 cm^{-1} (wide peak of O–H stretching overlapped with N–H stretching).
- The second vibration recorded between 2924 and 2820.8 cm^{-1} corresponds to (C–H stretching).
- The vibration is observed at 1640.03 and 1500 cm^{-1} corresponds to (amide II band, N–H bending, and C=O stretching of acetyl groups).
- A band relative to the carboxylic acid groups is manifested at 1085.96 cm^{-1}(bridge C–O–C stretching and C–O stretching).

Boehm titration

According to the experimental data obtained by the Boehm method, the quantities of acidic sites matching the carboxylic, phenolic, and lactonic sites and basic sites for *Pleurotus mutilus* biomass are presented in Table 1.

According to the analysis of experimental data using the Boehm method, which showed the existence of acidic

Table 1 Functional groups determined by Boehm method (Daoud et al. 2019)

Basic sites	Total acidic sites	Carboxylic	Phenolic	Lactonic
2.32 meq/g	4.33 meq/g	3.35 meq/g	0.46 meq/g	0.52 meq/g

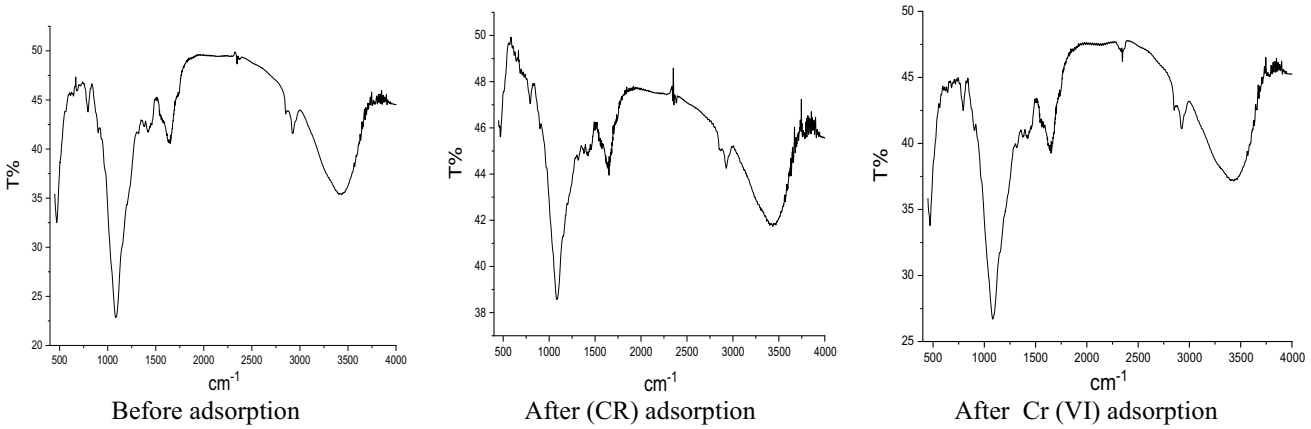

Fig. 2 Infrared spectrum of *Pleurotus mutilus* biomass

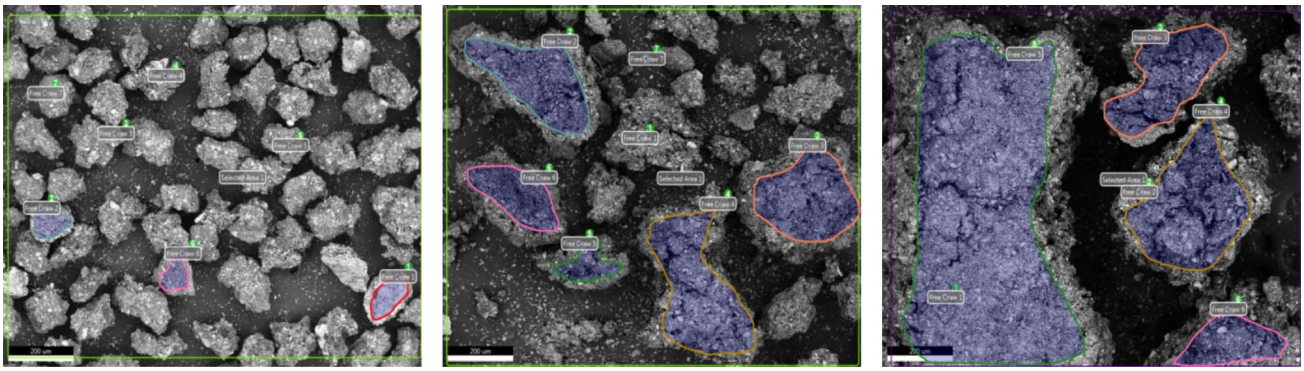

Fig. 3 Microphotographs of biosorbent particles for magnifications 100

Table 2 µXRF analysis of the mineral fraction of the biosorbent

Element	Ca	Si	P	Fe	K	Zn	Others
% (w/w)	42.9	36.9	13.4	4.1	2.3	0.2	0.2

and basic sites with the characteristics presented in Table 1 (Daoud et al. 2019), we concluded that the surface of *Pleurotus mutilus* biomass contains acidic and basic sites.

3.1.4. SEM micrographs observations

The SEM micrographs of the particles of the dried biosorbent reveal an outer microstructure of spherical shape having an almost smooth surface with the presence of cracks allowing easy adsorption of the solute, thereby improving the phenomenon of diffusion toward the active sites, Fig. 3.

TGA and XRF analyses

The µXRF spectrum of the mineral content, which represents 13.5% of the total weight of the sample, indicates the presence of metallic elements (Fe, Zn, Mo, Si) and calcium, phosphorus, and potassium. The residual elements are shown in Table 2. The three main elements (Ca, P, and K) are macronutrients, usually found in mushrooms (Guardia et al. 2005; Gençcelep et al. 2009). However, the existence of silicon with high calcium content is most probably due to contamination by the filtering agent that is used in the process of extracting *Pleuromutiline* which contains calcium carbonate powder and silica from diatomaceous soil.

Three peaks appear on the thermogram resulting from the TGA of the dried particles. The first peak at 50 °C is caused by the evaporation of the retained physisorbed water, involving a weight decrease of approximately 6%. Between the temperatures of 200 °C and 340 °C, appear the other remaining peaks, which correspond to the degradation of organic matter, that has the effect of losing 80% of the total weight of biomass according to (Moussous et al. 2012).

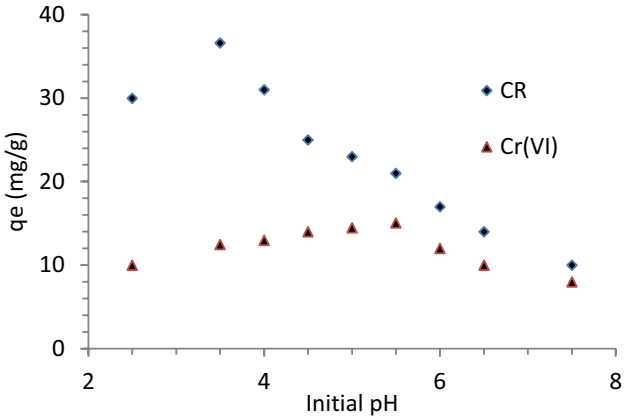

Fig. 4 Effect of initial pH

Effect of initial pH on metal ion biosorption

One of the important parameters affecting the biosorption capacity for the removal of metal ions and dye from aqueous solutions is pH values. Experiments were carried out in a pH range from 3 to 8 while maintaining the initial concentration of Cr (VI) ions and (CR) dye equal to 50 mg / L, a sorbent dose of 1 g/L. As shown in Figure 4, the optimal pH values, for the removal of Cr (VI) ions and (CR) dye, estimated are at pH 5.4 and 3.5, respectively.

The decreased sorption of Cr (VI) ions and the (CR) dye in alkaline media could be due to the decrease in

electrostatic attraction and the competitive biosorption between the OH^- ions and the anionic dye and ($HCrO_4^-$) ($CrO4^{-2}$) ions at the biosorption sites. In acidic environments, the low concentration of OH^- could be favorable to the biosorption of the negative ions on the biomass. A high electrostatic attraction could exist between the positively charged surface of the biosorbent and the anionic dye and ($HCrO_4^-$) ($CrO4^{-2}$) ions.

Furthermore, this result can be explained by the zero charge point (pHpzc) of the *Pleurotus mutilus* biomass, at which the electrical charge on the surface of the biosorbent is neutral. The overall charge of the biomass was positive in the acid pH values (pH < pH pzc). At pH < 7.94, the adhesion mechanism between biomass and pollutants is achieved by the electrostatic attraction of the $-NH_2$ amino groups present on the biomass' surface that come in the form of $-NH^{3+}$ (positively charged) and the Congo red and chromium ions pollutants charged negatively.

Study of initial concentration effect

Experimental adsorption capacities obtained are shown in Fig. 5, and the initial concentration for both pollutants varies between 25 and 150 mg/L. According to (Biswas et al. 2019) it is evident that increasing the initial concentration increases the adsorption capacity until a plateau is reached ($C_0 = 50$ mg/L, $q_{e,max}$ Cr(VI) = 15.08 mg/g, and $q_{e,max}$(CR) = 36.68 mg/g). This plateau is possibly due to the saturation of the binding sites (Bendjeffal et al. 2018). After occupying the active sites on the adsorbent, a dynamic equilibrium is established between the chromium ions, the Congo red dye, and the adsorbent surface (Rai et al. 2016). For the next phase of our tests, we have set at 50 mg/L as the initial concentration of Cr(VI) and (CR).

Kinetic studies

Many kinetic models have been proposed to elucidate the mechanism of adsorption and its potential rate-controlling steps that include mass transfer and chemical reaction processes.

Several kinetic models such as pseudo-first-order, pseudo-second-order, intraparticle diffusion, and Boyd models were commonly used to test the experimental data.

The pseudo-first-order kinetic model was proposed by Lagergren which is expressed using Eq. (6), according to (Ho and McKay 1999; Lagergren 1898):

$$\ln\left(q_e - q_t\right) = \ln\left(q_e\right) - K_1 t \tag{6}$$

The pseudo-second-order model is proposed by (Ho and McKay 1999), and based on the assumption that the adsorption follows second-order chemisorption, the pseudo-second-order model has the following form as presented in Eq. (7):

$$\frac{t}{q_t} = \frac{1}{K_2 q_e^2} + \frac{t}{q_e} \tag{7}$$

The experimental curves of Cr(VI) ions and (CR) dye uptake are shown in Fig. 6, and these results indicate that the uptake capacity stabilizes and reaches equilibrium after a time of 150 min for both pollutants. After this time, the equilibrium values obtained were $q_e = 15.08$ mg/g for chromium ions and $q_e = 36.68$ mg/g for Congo red dye.

The ionic form of Cr(VI) in solution and the biomass ionization degree are significantly related to the pH solution. Ionic forms of chromium, i.e., $HCrO_4^-$, $Cr_2O_7^{2-}$ and CrO_4^{2-}, are present for the range of 3.5 < pH < 5.5 according to (Rangabhashiyam and Balasubramanian 2018). Congo red is known to be an anionic dye. The pHzpc value obtained was 7.94.

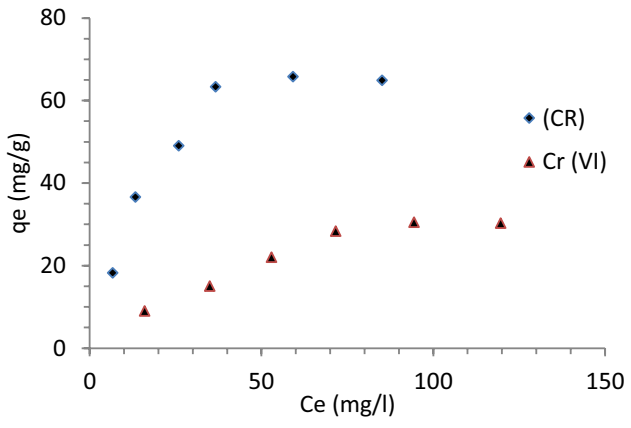

Fig. 5 Initial concentration effect on equilibrium biosorption capacity q_e

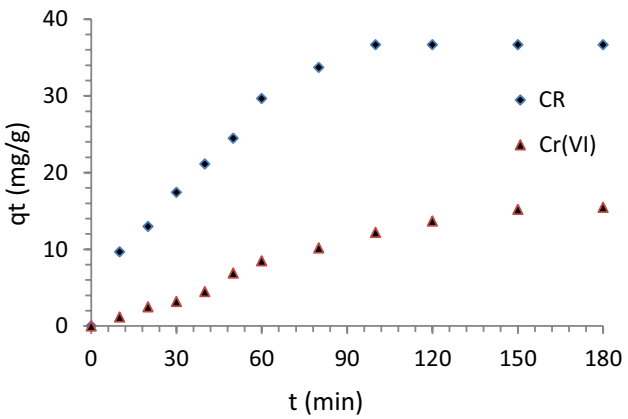

Fig. 6 Contact time effect on biosorption capacity

Therefore, at a pH value below 7.94, the surface area of *Pleurotus mutilus* biomass is positively charged. The binding of the negatively charged chromium ions and Congo red dye to the surface of the positively charged *Pleurotus mutilus* biomass takes place by electrostatic attraction.

The adsorption of (CR) dye and the Cr(VI) ions on the biomass is rapid up to 150 min, according to the experimental kinetic curves shown in Fig. 6. In later phases, after 150 min adsorption became slower and it took longer to adsorb the two pollutants due to the decrease in these active sites (Dautoo et al. 2017). After this time, the curve reaches a plateau, indicating that the biosorption equilibrium has been achieved for both pollutants. The pseudo-first-order parameters, *qe* and K_1, were calculated based on Fig. 7, while those of pseudo-second-order, *qe* and K_2 were estimated from another figure, using the formula $t/q_t = f(t)$, not presented in this paper. These values are summarized in Table 3.

The pseudo-first-order model well describes the experimental kinetic data indicated by the analysis of the experimental results shown in Table 3 where $R^2 > 0.95$ for both (CR) dye and Cr(VI) ions.

Intraparticle mass transfer (Weber and Morris)

Weber and Morris (Weber 1963) proposed a model represented by Eq. (8). This model will be applied to the experimental kinetic data to estimate the intraparticle diffusion coefficient. It can describe the mechanisms and steps for controlling the rate that influences adsorption kinetics (Nakkeeran and Selvaraju 2017).

$$q_t = K_i.t^{0.5} \tag{8}$$

Taking into account only the initial period in Weber and Morris model, the diffusion coefficient D_w in the solid phase can be estimated by using Eq. (9) according to (Selatnia et al. 2004)

$$K_i = \left(\frac{12q_e}{d_p}\right)\left(\frac{D_w}{\pi}\right)^{0.5} \tag{9}$$

The value of the diffusion coefficient can be calculated by using the first line in Fig. 8, which gives values in the range of 4.81 10^{-14} m^2/s for Cr(VI) ions and 1.11 10^{-13} m^2/s for (CR) dye. The intraparticle diffusion coefficient can be estimated by using another model as Urano and Tachikawa model.

Intraparticle mass transfer (Urano and Tachikawa model)

It has been proposed by (Urano and Tachikawa 1991) which is an intraparticle diffusion model, where external diffusion has been neglected due to the low adsorption rate, and the

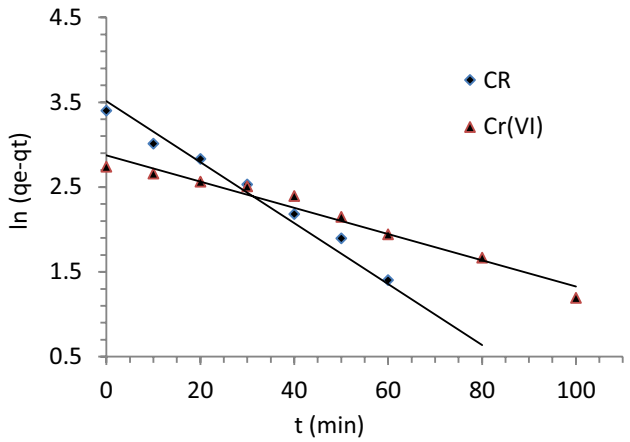

Fig. 7 Application of the pseudo-first-order model to experimental kinetic results

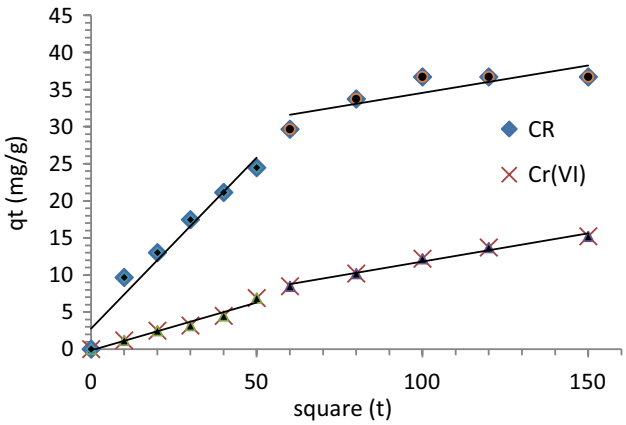

Fig. 8 Application of Weber and Morris model

Table 3 Kinetics parameters for biosorption

Pseudo-first-order				Pseudo-second-order			
Parameter	q_e (mg/g) (experimental)	q_e (mg/g) (model)	K_1 (min^{-1})	R^2	q_e (mg/g) (model)	K_2 ($g.mg^{-1}$ min^{-1})	R^2
(CR) dye	36.68	42.14	0.035	0.977	62.50	2.28 10^{-4}	0.936
Cr(VI)	15.50	17.32	0.015	0.954	66.66	3.41 10^{-5}	0.423

agitation is considered independent of the adsorption rate (Anirudhan and Suchithra 2008), biosorption kinetics were modeled by Eq. (10):

$$-\ln\left[1-\left(q_t/q_e\right)^2\right]=\frac{4\pi^2 D_i t}{d_p^2} \tag{10}$$

The mean diffusion coefficient in solid D_i (m^2/s) has been calculated by plotting $-\ln\left[1-\left(q_t/q_e\right)^2\right]$ versus time (t). The intraparticle diffusion coefficient may be calculated according to Fig. 9, which gives values in the range of $4.93.10^{-12}$ m^2/s for Cr(VI) ions and $1.48.10^{-11}$ m^2/s for (CR) dye. These values are lower than the diffusion coefficient of the species in solution (10^{-9} m^2/s), suggesting that intraparticle diffusion can be considered negligible compared to the external mass transfer from the liquid film onto the solid particle.

Boyd model

As a result of the dual dependence of the adsorption rate on the uptake mechanism (Khalid et al. 2017) which is either film or intraparticle diffusion (Rangabhashiyam and Selvaraju 2015), Boyd's model has been applied to the experimental data for identifying the limiting step (Khalid et al. 2018; Boyd 1947). According to (Aravindhan et al. 2009), the kinetic expression of this model has been reported as follows:

$$B_t = -0.4977 - \ln(1-F) \tag{11}$$

The rate of biosorption consists of three stages, namely, the diffusion in the film surrounding the solid particle of the adsorbent (external mass transfer), followed by an intraparticle mass transfer (inside the pores of the particle), and finally the adsorption on the solid which is generally assumed to be rapid. The application of the Boyd model to experimental kinetic data makes it possible to conclude whether intraparticle mass transfer or external mass transfer controls the biosorption rate according to (Khalid et al. 2018; Boyd 1947). After fitting the equilibrium data to Boyd's model by plotting (B_t) versus time (t), according to Fig. 10 we can see that the line obtained does not pass through the origin (John Babu et al. 2019); this allowed us to verify that the rate-controlling step is governed by film diffusion. The given relation presented in Eq. (10) is used to determine the value of diffusion coefficient D_j according to (Khalid et al. 2017):

$$B_t = \left(\frac{\pi^2}{r_p^2}D_j\right)\times t \tag{12}$$

where r_p is the radius of biomass particles, and the value of diffusion coefficient (D_j) for both pollutants is of the order of $1.79\ 10^{-13}$ m^2/s for Cr(VI) ions and $4.79\ 10^{-13} m^2/s$ for (CR) dye. Otherwise, these values are lower than the diffusion coefficient of species in solution (10^{-9} m^2/s).

Therefore, we can conclude that the intraparticle mass transfer (internal mass transfer) is negligible compared to external mass transfer and consequently the diffusion through the liquid film surrounding the particle (external mass transfer) controls the biosorption rate (Aravindhan et al. 2009).

Adsorption isotherms

Different models of adsorption isotherms, namely Langmuir, Freundlich, Temkin, and finally Dubinin-Radushkevich, were used for simulating the experimental equilibrium values of adsorption equilibrium of (CR) dye and Cr(VI) ions onto *Pleurotus mutilus* biomass.

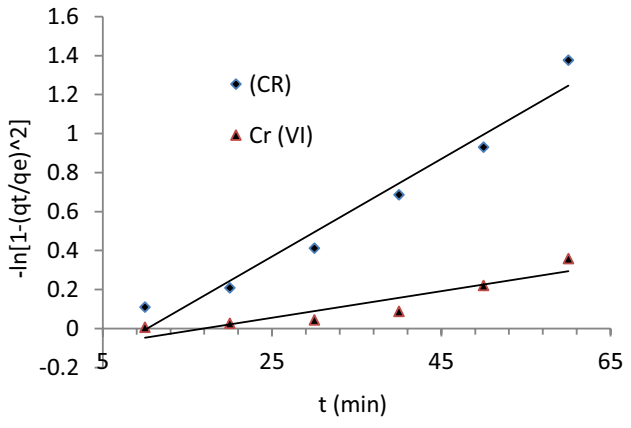

Fig. 9 Application of Urano and Tachikawa model to experimental data

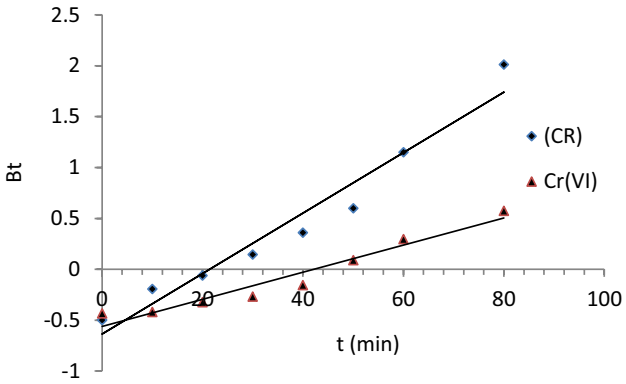

Fig. 10 Application of Boyd model to experimental data

Langmuir model

Removal of Cr(VI) and (CR) was described by this model as single-layer adsorption on a uniform surface, where there are no adsorbate interactions at adjacent sites (Langmuir 1918). The Langmuir isotherm is presented by a linear model as follows:

$$\frac{C_e}{q_e} = \frac{1}{q_m b} + \frac{C_e}{q_m} \tag{13}$$

The coefficient b, as well as the maximum capacity q_m, may be determined according to the graph representing $\frac{C_e}{q_e}$ versus C_e (not shown here). The distribution factor R_L presented in Eq. (14) can describe the characteristics and type of the Langmuir isotherm.

$$R_L = \frac{1}{1 + bC_0} \tag{14}$$

Further analysis can be made according to the R_L value. A favorable adsorption process is dominant for R_L varying between 0 and 1. While adsorption is linear when $R_L = 1$, unfavorable is for $R_L > 1$, it will be irreversible, in the case where $R_L = 0$, (Dubey and Gopal 2009; Rai et al. 2016; Rezaei 2016).

Given the results of the Langmuir parameter calculation shown in Table 4, we can conclude that the Langmuir model inadequately predicts the experimental equilibrium values for (CR) dye and Cr(VI) ions according to the obtained values of R^2, χ^2 and ARE. The adsorption process is favorable ($0 < R_L < 1$) for both pollutants (Mohagheghian et al. 2017; Yang et al. 2016).

Freundlich model

Different energies of the active sites are involved, according to the hypothesis of heterogeneity of the adsorption surface (Qu et al. 2015). The Freundlich isothermal model is applied to experimental data, which is expressed according to the following equation:

$$\ln q_e = \ln K_F + \frac{1}{n}\ln C_e \tag{15}$$

The plot of $\ln q_e$ versus $\ln C_e$ shown in Fig. 11 gives a straight line with a slope (1/n) which represents the intensity of adsorption for the Freundlich model. This exponent is lower for more heterogeneous surfaces (Doke et al. 2013). The results presented in Table 4 illustrate clearly that the Freundlich model represents the experimental equilibrium values for Cr(VI) ions and the (CR) dye based on R^2, χ^2, and ARE values.

Table 4 Isothermal parameters for (CR) dye and Cr(VI) ions biosorption onto *Pleurotus mutilus* biomass

Isotherm model	Equation	Parameter	Unit	(CR)	Cr(VI)
Langmuir	$\frac{C_e}{q_e} = \frac{1}{q_m b} + \frac{C_e}{q_m}$	q_m	(mg/g)	83.33	90.9
		b	(L/mg)	0.050	0.039
		R^2	–	0.975	0.930
		R_L	–	0.591	0.286
		χ^2	–	38.86	338.04
		ARE	–	25.96	189.07
Freundlich	$\ln q_e = \ln K_F + \frac{1}{n}\ln C_e$	$1/n$	–	0.642	0.720
		K_f	–	5.387	1.221
		R^2	–	0.934	0.988
		χ^2	–	16.33	2.33
		ARE	–	14.92	7.76
Temkin	$q_e = (\mathrm{RT}/B)\ln K_T + (\mathrm{RT}/B)\ln C_e$	K_T	(L/g)	0.464	0.114
		B	(J/mol)	127.84	195.77
		R^2	–	0.929	0.963
		χ^2	–	3.78	1.54
		ARE	–	8.37	8.75
Dubinin-Radushkevich	$\ln q_e = \ln q_{\max} - \beta \in^2$ $E = \frac{1}{\sqrt{2\times\beta}}$	$q_{\max}$	(mg/g)	40.44	17.63
		β	($\mathrm{mol^2/J^2}$)	1.10^{-5}	6.10^{-5}
		E	(kJ/mol)	0.111	0.168
		R^2	–	0.944	0.992
		χ^2	–	35.81	21.33
		ARE	–	32.35	37.26

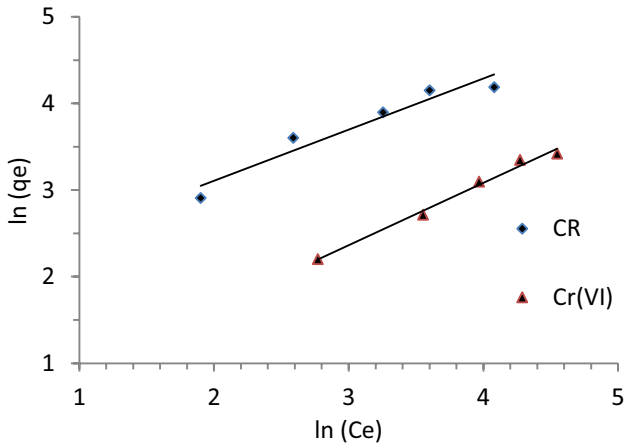

Fig. 11 Freundlich model plot

Temkin model

The adsorbant–adsorbate interactions are the basis of the Temkin isotherm hypothesis. The decrease in biosorption heat changes linearly with the coverage (Liu and Liu 2008). This model can be presented using the linearized form in Eq. (16) as follows:

$$q_e = (\mathrm{RT}/B)\ln K_T + (\mathrm{RT}/B)\ln C_e \tag{16}$$

We deduce the values of K_T and B from the straight line representing (q_e) as a function of ln(Ce). Temkin parameters are presented in Table 4. It can be concluded that increasing biosorbent coverage leads to a decrease in biosorption heat.

From the results obtained, we can see that the value of B (J/mol) is less than 8 kJ/mol. This leads us to conclude that the adsorption process of chromium ions and (CR) dye is a physical process in nature (physisorption).

The Dubinin-Radushkevich model

The physical or chemical character of the biosorption is identified by applying the Dubinin-Radushkevich model (Fontana et al. 2016) as indicated in Eq. (17)

$$\ln q_e = \ln q_{\max} - \beta \in^2 \tag{17}$$

where β is a constant that depends on E (adsorption energy in J/mol). Equation (18) may be used for the calculation of the parameter ε as follows:

$$\varepsilon = \mathrm{RT}\ln\left(1 + \frac{1}{C_e}\right) \tag{18}$$

The plot of $\ln(q_e)$ versus (ϵ^2) not shown here allows the calculation of β and therefore the value of E by using Eq. (19):

$$E = \frac{1}{\sqrt{2 \times \beta}} \tag{19}$$

The adsorption process is predicted by calculating the value of the adsorption energy E (Liu and Liu 2008). For the physisorption process, the value of the average adsorption energy is between 0 and 8 kJ/mol. For the chemisorption process, the value is in the range of 8 to 16 kJ/mol; in case this energy is higher than 16 kJ/mol the particle diffusion dominates the adsorption process (Daoud et al. 2019). The Dubinin-Radushkevich parameters can be seen in Table 4.

Adsorption energy values E for chromium ions and Congo red dye are below 8 kJ/mol, indicating that the adsorption mechanism is physical in nature according to Temkin and Dubinin-Radushkevich models. By comparing the maximum of biosorption capacity on *Pleurotus mutilus* biomass obtained for the removal of (CR) dye and Cr(VI) ions with our results on other biosorbents (Table 5), it appears that *Pleurotus mutilus* biomass has an acceptable potential for recovery (CR) dye and Cr(VI) ions from dilute solutions (Co < 50 mg/L).

Study of the temperature effect

The biosorption of chromium ions and Congo red dye on *Pleurotus mutilus* biomass was investigated under optimal conditions of pH and initial concentration for both pollutants. This was done for different temperatures from 308 to 318 K. To assess the feasibility of the process from a thermodynamic point of view, the values of the free energy ΔG°, entropy ΔS°, enthalpy ΔH° were calculated using Eq. (20) and Eq. (21) (Selmi 2018).

$$\ln K_L = -\frac{\Delta H^\circ}{RT} + \frac{\Delta S^\circ}{R} \tag{20}$$

$$\Delta G^\circ = \Delta H^\circ - T\Delta S^\circ \tag{21}$$

where $K_L = q_e/C_e$ is the equilibrium constant (Jayakumar et al. 2014; Khelaifia et al. 2016). From Eq. (20) and by plotting the curve ln K_L versus $1/T$, we can deduce the values of $\Delta H°$ and ΔS° as presented in Table 5. The obtained results suggest that the binding processes for Cr(VI) ions are endothermic $\left(\Delta H^\circ > 0\right)$ according to (Jayakumar et al. 2014; Khelaifia et al. 2016) and exothermic for (CR) dye. The increase in temperature facilitates the adsorption of Cr(VI) ions according to (Jayakumar et al. 2014; Khelaifia et al. 2016), whereas the uptake will be not favored by an increase in temperature for (CR) dye removal and there is an increase in disorder ($\Delta S^\circ > 0$) according to (Wang et al.

Table 5 Comparison of hexavalent chromium and Congo red biosorption capacity for different biosorbents

Biosorbent	Biosorbent capacity q_{max}(mg/g)	References
Hexavalent chromium Cr (VI)		
Pleurotus mutilus	15.08	This study
Pleurotus mutilus	29.40	(Alouache et al. 2017)
Natural foxtail millet shell	11.70	(Peng et al. 2018)
Agave sisalana fibers	58.60	(Bendjeffal et al. 2018)
Powdered Cotton Stalk	35	(Doke et al. 2013)
Rutin resin	41.6	(Fathy et al. 2015)
Marine green algae *Halimeda gracilis*	55.55	(Jayakumar et al. 2014)
Gracilaria corticata (Red Algae)	4.98	(Kavitha et al. 2016)
Acacia nilotica	8.20	(Khalid et al. 2018)
Raw biomaterial waste-date stones	70	(Khelaifia et al. 2016)
Scallop shell-Fe3O4 nanoparticles	34.48	(Mohagheghian and Vahidi-Kolur 2017)
Strychnine tree fruit shell	142.85	(Nakkeeran and Selvaraju 2017)
Magnolia leaf biomass	3.96	(Kumar et al. 2019)
Congo red dye (CR)		
Pleurotus mutilus	36.68	This study
Wheat bran	22.73	(Wang and Chen 2009)
Pine cone	40.19	(Dawood and Sen 2012)
Sugarcane bagasse	38.2	(Zhang et al. 2011)
Aspergillus carbonarius	99.01	(Bouras et al. 2017)
Penicilium glabrum	101.01	(Bouras et al. 2017)
Orange peel	22.4	(Namabsivayam et al. 1996)
*Penicllium*sp.YW01	411.53	(Yang et al. 2011)
Cabbage waste powder	1.6	(Wekoye et al. 2020)
Cattail root	38.79	(Hu et al. 2010)

Table 6 Thermodynamic biosorption values of hexavalent chromium ions and Congo red dye

Temperature (K)	Congo red biosorption			Chromium biosorption		
	ΔG°	ΔH°	ΔS°	ΔG°	ΔH°	ΔS°
300	− 2.61	− 46.44	146.00	− 0.23	24.40	82.10
308	− 1.44			− 0.88		
313	− 0.71			− 1.30		
318	− 0.02			− 1.70		

2012). The adsorption process of hexavalent chromium ions and Congo red dye is spontaneous according to the negative values of ΔG° presented in Table 6.

Desorption study

The recycling of the adsorbent through the desorption process is the most important aspect from an economic point of view. Desorption is an indispensable part of the adsorption process. The aim is to estimate the reuse of any adsorbent industrially, for ecological interests and sustainable development (Bessaha et al. 2019).

In addition, the process allows the adsorbents to be regenerated each time so that they can be used in several adsorption–desorption cycles. The recovery of the metal or dye extracted from the liquid phase can be made through the desorption process which significantly reduces the cost of treatment (Jayakumar et al. 2014; Pathania et al. 2016). After the adsorption process, the biomass is recovered by filtration. The desorption was achieved by introducing a known amount of biomass loaded with Cr(VI) ions or (CR) dye into a 50-mL beaker. The Cr(VI) ions were treated with HNO_3 and (CR) dye with C_2H_5OH (Bessaha et al. 2019). The contents are kept under stirring for 1 h. After the desorption process, the liquid solution is separated from the biomass

by filtration; then, the biomass was regenerated without any load on the environment in terms of disposal (Fathy et al. 2015). The resulting filtrate containing (CR) dye or Cr(VI) ions shows that 80% of the adsorbed (CR) dye and 90% of the adsorbed Cr(VI) ions have been recovered after regeneration; this operation enables reduction of volumes of pollution. These satisfactory preliminary results allow us to plan further tests on the adsorption–desorption cycle to define how many cycles the *Pleurotus mutilus* biomass can be reused. The results obtained will be reported in another work.

Simultaneous adsorption of hexavalent chromium and Congo red dye

The adsorption mechanism of (CR) and Cr(VI) on biomass has been complicated and affected by various interactions, such as ion exchange, functional groups, and π–π interaction between biomass and adsorbates (Mahmoudi et al. 2020). The attractive force between the negatively charged contaminants and the positively charged biomass according to the pHzpc value can further explain the adsorption of (CR) and Cr(VI). The binary adsorption potential of *Pleurotus mutilus* toward CR and Cr(VI) is illustrated in Fig. 12. The percentage of removal for solution 1 (30% (CR) and 70% Cr(VI)) for (CR) and Cr(VI) was estimated 28.4% and 30.2%, respectively. When passing from solution 2 to solution 3 of the binary mixture, the percentages of dye removal (CR) increased from 51.8 to 73.0%, while those of Cr (VI) decreased from 26.7 to 24.0%, respectively.

However, contrary to the Congo red removal, the removal of hexavalent chromium was not as high, and the same observations have been reported by (Kumari et al. 2018; Mahmoudi et al. 2020).

In the binary mixture solution, a competition was observed between (CR) and Cr(VI) to be adsorbed on the Pleurotus mutilus biomass. (CR) can efficiently be more adsorbed by free sites and adsorbent functional groups. But there was no race between (CR) and Cr(VI) in the adsorption batch of the single solution, while the free functional groups were linked with the single adsorbate (Mahmoudi et al. 2020).

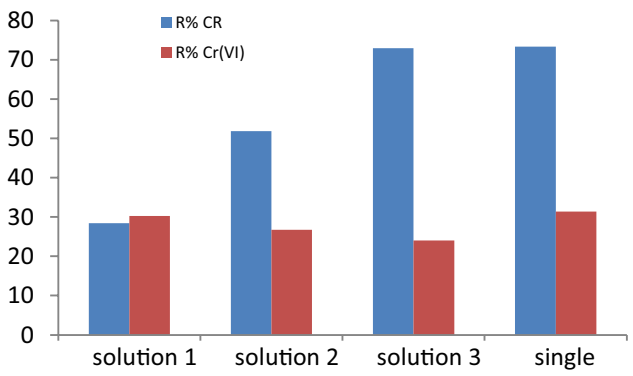

Fig. 12 Binary adsorption of (CR) and Cr(VI) by *Pleurotus mutilus* at different ratios of solution concentration

The biomass of *Pleurotus mutilus* was capable of simultaneously removing both pollutants CR and Cr (VI). In this experiment, CR was more effectively eliminated than Cr (VI). Neither CR nor Cr(VI) have been completely removed in the case of simultaneous removal. Under the operating conditions adopted, i.e., room temperature, 20 °C and a pH value equal to 5, the maximum elimination percentages were of the range of 73% for (CR) dye and 30.2% for Cr (VI) ions. The results obtained for the simultaneous mixing of the two pollutants are comparable with the case of a single treatment of each pollutant, in which the elimination percentages were 73.4% and 31.4% for (CR) and Cr (VI), respectively.

Conclusion

This research aimed first and foremost to evaluate the capacity of *Pleurotus mutilus* biomass to be a natural, environmentally friendly, and inexpensive biosorbent for the treatment of pollutants in wastewater. The removal of hexavalent chromium ions and Congo red dye using pharmaceutical industry waste, substituting the very expensive process of pollutant removal, showed prominent results as the biosorption capacities were 36.68 mg/g for the dye (CR) and 15.08 mg/g for Cr(VI) ions. This biomass has been successfully able to remove both Congo red and chromium simultaneously with higher efficiency of Congo red elimination.

Modeling of these experimental kinetic data indicated that the pseudo-first-order kinetic model matched well with the experimental results for Cr(VI) ions and (CR) dye.

Experimental data applied to diffusion models such as Weber-Morris, Urano-Tachikawa, and Boyd models demonstrate that external mass transfer is the dominating process controlling the biosorption rate of (CR) dye and Cr(VI) ions on the *Pleurotus mutilus* biomass.

The adsorption is multilayer and physical in nature according to adsorption isotherms models of Freundlich, Temkin, and Dubinin-Radushkevich. The values of ΔG^{o} and ΔH^{o} indicated a spontaneous and physical biosorption in nature. The (CR) dye and Cr(VI) ions biosorption are exothermic and endothermic, respectively, according to the obtained ΔH^{o} values.

The results of this research are glaring evidence that *Pleurotus mutilus* biomass (waste originally destined for incineration) can be considered as a cost-effective source for the removal of (CR) and Cr(VI) from contaminated waters. Low-cost adsorbents used in biosorption and might be sustainable, feasible, and economically exploitable technology.

The recycling process using C_2H_5OH and HNO_3 solutions has achieved regeneration rates of approximately 80% for (CR) dye and 90% for Cr(VI) ions, respectively. It reduces the cost and opens the capability of recovering the metal or dye extracted out of the liquid phase.

Therefore, the importance of these studies for the practical and economical use of biosorbents that prohibit the treatment of dilute wastewater containing (CR) dye and Cr(VI) ions is quite clear.

The increase in the removal of Cr(IV) ions and (CR) dye by chemically modified *Pleurotus mutilus* biomass or biochar would be the next step in our research and preliminary results so far exhibited satisfactory results and will be reported on other works.

Acknowledgements The authors thank the financial contribution of DGRSDT and PRFU project in national polytechnical school (comparative study of adsorption of dyes and heavy metal, organic compounds on different types of adsorbents) with code A16N01ES160220180002 of 01/01/2018.

References

Afroze S, Sen TK (2018) A review on heavy metal ions and dye adsorption from water by agricultural solid waste adsorbents. Water Air Soil Pollut 229:225

Ajmani A, Shahnaz T, Narayanan S, Narayanaswamy S (2019) Equilibrium, kinetics and thermodynamics of hexavalent chromium biosorption on pristine and zinc chloride activated Senna siamea seed pods. Chem Ecol 35(4):379–396. https://doi.org/10.1080/02757540.2019.1584614

Alouache A, Selatnia A, Halet F (2017) "Biosorption of Cr (VI) from aqueous solutions by dead biomass of pleurotus mutilus in torus reactor" in Frontiers in wastewater treatment and modelling. [online] http://link.springer.com/https://doi.org/10.1007/978-3-319-58421-8

Anirudhan TS, Suchithra PS (2008) Synthesis and characterization of tannin-immobilized hydrotalcite as a potential adsorbent of heavy metal ions in effluent treatments. Appl Clay Sci 42(1–2):214–223. https://doi.org/10.1016/j.clay.2007.12.002

Aravindhan R, Rao JR, Nair BU (2009) Application of a chemically modified green macro alga as a biosorbent for phenol removal. J Environ Manage 90(5):1877–1883

Bendjeffal H, Djebli A, Mamine H, Metidji T, Dahak M, Rebbani N, Bouhedja Y (2018) Effect of the chelating agents on bio-sorption of hexavalent chromium using Agave sisalana fibers. Chin J Chem Eng. https://doi.org/10.1016/j.cjche.2017.10.016

Bessaha F, Mahrez N, Marouf-Khelifa K, Çoruh A, Khelifa A (2019) Removal of Congo red by thermally and chemically modified halloysite: equilibrium, FTIR spectroscopy, and mechanism studies. Int J Environ Sci Technol 16(8):4253–4260. https://doi.org/10.1007/s13762-018-2041-z

Biswas S, Meikap BC, Sen TK (2019) Adsorptive removal of aqueous phase copper (Cu^{2+}) and Nickel (Ni^{2+}) Metal Ions by synthesized biochar–biopolymeric hybrid adsorbents and process optimization by Response Surface Methodology (RSM). Water Air and Soil Pollut 230:197https://doi.org/10.1007/s11270-019-4258-y

Blanes PS, Bordoni ME, González JC, García SI, Atria AM, Sala LF, Bellú SE (2016) Application of soy hull biomass in removal of Cr(VI) from contaminated waters. Kinetic, thermodynamic and continuous sorption studies. J Environ Chem Eng 4(1):516–526. https://doi.org/10.1016/j.jece.2015.12.008

Boehm HP (1994) Some aspects of the surface chemistry of carbon blacks and other carbons. Carbon 32(5):759–769

Bouras HD, Yeddou AR, Bouras N, Hellel D, Holtz MD, Sabaou N, Chergui A, Nadjemi B (2017) Biosorption of Congo red dye by Aspergillus carbonarius M333 and Penicillium glabrum Pg1: Kinetics, equilibrium and thermodynamic studies. J Taiwan Inst Chem Eng 80:915–923. https://doi.org/10.1016/j.jtice.2017.08.002

Boyd GE, Adamson AW, Myers LS (1947) The exchange adsorption of ions from aqueous solutions by organic zeolites. II. Kinetics. J Am ChemSoc 69:2836–2848

Chang C (2019) Agricultural waste. Water Environ Res 2018:1150–1167

Chatterjee S, Shekhawat K, Gupta N (2019) Bioreduction of toxic hexavalent chromium by novel indigenous microbe Brevibacillus agri isolated from tannery wastewater. Int J Environ Sci Technol 16:3549–3556

Chauhan D, Afreen S, Mishra S, Sankararamakrishnan N (2017) Journal of Industrial and Engineering Chemistry Synthesis, characterization and application of zinc augmented aminated PAN nano fibers towards decontamination of chemical and biological contaminants. J Ind Eng Chem 55:50–64.https://doi.org/10.1016/j.jiec.2017.06.027

Cherifi H, Bentahar F, Hanini S (2014) Biosorption of phenol by dried biomass. Desalin Water Treat 52(7-9):1699–1704

Daoud N, Selatnia A, Benyoussef EH (2019) Nickel removal from aqueous solution by non-living Pleurotus mutilus: kinetic, equilibrium, and thermodynamic studies. Algerian J Environ Sci Technol 4(3):1–14

Dautoo UK, Shandil Y, Chauhan GS (2017) New crosslinked hydrazide–based polymers as Cr(VI) ions adsorbents. J Environ Chem Eng 5(6):5815–5826

Dawood S, Sen TK (2012) Removal of anionic dye Congo red from aqueous solution by raw pine and acid-treated pine cone powder as adsorbent: Equilibrium, thermodynamic, kinetics, mechanism and process design. Water Res 46(6):1933–1946. https://doi.org/10.1016/j.watres.2012.01.009

Dermatas D, Mpouras T, Chrysochoou M, Panagiotakis I, Vatseris C, Linardos N, Theologou E, Boboti N, Xenidis A, Papassiopi N, Sakellariou L (2015) Origin and concentration profile of chromium in a Greek aquifer. J Hazard Mater 281:35–46. https://doi.org/10.1016/j.jhazmat.2014.09.050

Doke K, Khan E, Gaikwad V (2013) Diffusion mechanisms of biosorption of Cr(VI) onto powdered cotton stalk. J Dispers Sci Technol 34(10):1347–1355

Dubey SP, Gopal K (2009) Application of natural adsorbent from silver impregnated Arachis hypogaea based thereon in the processes of hexavalent chromium for the purification of water. J Hazard Mater 164(2–3):968–975

Fathy NA, El-Wakeel ST, Abd El-Latif RR (2015) Biosorption and desorption studies on chromium(VI) by novel biosorbents of raw rutin and rutin resin. J Environ Chem Eng 3(2):1137–1145. https://doi.org/10.1016/j.jece.2015.04.011

Fidel RB, Laird DA, Thompson ML (2013) Evaluation of modified boehm titration methods for use with biochars. J Environ Qual 42(6):1771–1778

Fontana KB, Chaves ES, Sanchez JDS, Watanabe ERLR, Pietrobelli JMTA, Lenzi GG (2016) Ecotoxicology and environmental safety textile dye removal from aqueous solutions by malt bagasse : Isotherm, kinetic and thermodynamic studies. Ecotoxicol Environ Safety 124:329–336. https://doi.org/10.1016/j.ecoenv.2015.11.012

Foroughi-Dahr M, Abolghasemi H, Esmaili M, Shojamoradi A, Fatoorehchi A (2014) Adsorption characteristics of congo red

from aqueous solution onto tea waste. Chem Eng Commun 202(2):181–193
Gençcelep H, Uzun Y, Tunçtürk Y, Demirel K (2009) Determination of mineral contents of wild-grown edible mushrooms. Food Chem 113:1033–1036
Ghaneian MT, Bhatnagar A, Ehrampoush MH (2017) Biosorption of hexavalent chromium from aqueous solution onto pomegranate seeds: kinetic modeling studies. Int J Environ Sci Technol 14:331–340
Ghuge SP, Saroha AK (2018) Catalytic ozonation of dye industry effluent using mesoporous bimetallic Ru-cu/SBA-15 catalyst. Process Saf Environ Prot 118:125–132
Guardia ML, Venturella G, Venturella F (2005) On the chemical composition and nutritional value of Pleurotus taxa growing on umbelliferous plants (Apiaceae). J Agric Food Chem 53:5997–6002
Gupta VK, Suhas (2009) Application of low-cost adsorbents for dye removal–A review. J Environ Manage 90(8):2313–2342. https://doi.org/10.1016/j.jenvman.2008.11.017
Hafiane A, Lemordant D, Dhahbi M (2000) Removal of hexavalent chromium by nanofiltration. Desalination 130(3):305–312
Ho YS, McKay G (1999) Pseudo-second order model for sorption processes. Process Biochem 34(5):451–465
Hu Z, Chen H, Ji F, Yuan S (2010) Removal of Congo red from aqueous solution by cattail root. J Hazard Mater 173(1–3):292–297
Jayakumar R, Rajasimman M, Karthikeyan C (2014) Sorption of hexavalent chromium from aqueous solution using marine green algae Halimeda gracilis : optimization, equilibrium, kinetic, thermodynamic and desorption studies. J Environ Chem Eng 2(3):1261–1274. https://doi.org/10.1016/j.jece.2014.05.007
John Babu D, King P, Prasanna Kumar Y (2019) Optimization of Cu (II) biosorption onto sea urchin test using response surface methodology and artificial neural networks. Int J Environ Sci Technol 16(4):1885–1896. https://doi.org/10.1007/s13762-018-1747-2
Kavitha G, Sridevi V, Venkateswarlu P, Babu NC (2016) Biosorption of chromium from aqueous solution by gracilaria corticata (Red Algae) and its statistical analysis using response surface methodology. **3**(Ccd)
Khalid R, Aslam Z, Abbas A, Ahmad W, Ramzan N, Shawabkeh R (2017) Adsorptive potential of Acacia Nilotica based adsorbent for Chromium (VI) from an aqueous phase. Chin J Chem Eng. https://doi.org/10.1016/j.cjche.2017.08.017
Khalid R, Aslam Z, Abbas A, Ahmad W, Ramzan N (2018) Adsorptive potential of Acacia nilotica based adsorbent for chromium(VI) from an aqueous phase. Chin J Chem Eng 26:614–622
Khelaifia FZ, Hazourli S, Nouacer S, Rahima H, Ziati M (2016) Valorization of raw biomaterial waste-date stones-for Cr (VI) adsorption in aqueous solution: thermodynamics, kinetics and regeneration studies. Int Biodeterior Biodegradation 114:76–86
Khitous M, Salem Z, Halliche D (2016) Sorption of Cr(VI) by MgAl-NO3 hydrotalcite in fixed-bed column: experiments and prediction of breakthrough curves. Korean J Chem Eng 33(2):638–648
Kongsricharoern N, Polprasert C (1996) Chromium removal by a bipolar electro-chemical precipitation process. Water Sci Technol 34(9):109–116
Kumar N, Angela M, Palas S, Biswajit R (2019) Optimization study of adsorption parameters for removal of Cr (VI) using Magnolia leaf biomass by response surface methodology. Sustain Water Resour Manag (Vi). https://doi.org/10.1007/s40899-019-00322-5
Kumari D, Mazumder P, Kumar M, Deka JP, Shim J (2018) Simultaneous removal of Cong red and Cr (VI) in aqueous solution by using Mn powder extracted from battery waste solution. Groundwater Sustain Develop. https://doi.org/10.1016/j.gsd.2018.01.001
Lagergren S (1898) About the theory of so-called adsorption of soluble substances, Kungliga Svenska Vetenskapsakademien. Handlingar 24:1–39
Langmuir I (1918) The adsorption of gases on plane surfaces of glass, mica and platinum. J Am Chem Soc 40(9):1361–1403
Liu Y, Liu YJ (2008) Biosorption isotherms, kinetics and thermodynamics. Sep Purif Technol 61(3):229–242
Mahmoudi E, Azizkhani S, Mohammad AW, Ng LY, Benamor A, Ang WL, Ba-Abbad M (2020) Simultaneous removal of Congo red and cadmium (II) from aqueous solutions using graphene oxide–silica composite as a multifunctional adsorbent. J Environ Sci (China) 98:151–160
Mohagheghian A, Vahidi-Kolur R (2017) Application of Scallop shell-Fe 3 O 4 nanoparticles for the removal of Cr(VI) from aqueous solutions. Water Sci Technol 75(10):2369–2380
Mohagheghian A, Vahidi-Kolur R, Pourmohseni M, Yang JK, Shirzad-Siboni M (2017) Application of scallop shell-Fe3O4 nanoparticles for the removal of Cr(VI) from aqueous solutions. Water Sci Technol 75(10):2369–2380
Moussous S, Selatnia A, Merati A, Junter GA (2012) Batch cadmium(II) biosorption by an industrial residue of macrofungal biomass (Clitopilus scyphoides). Chem Eng J 197:261–271. https://doi.org/10.1016/j.cej.2012.04.106
Nadeem K, Guyer GT, Keskinler B, Dizge N (2019) Investigation of segregated wastewater streams reusability with membrane process for textile industry. J Clean Prod 228:1437–1445
Nakkeeran E, Selvaraju N (2017) Biosorption of Chromium (VI) in aqueous solutions by chemically modified Strychnine tree fruit shell. International Journal of Phytoremediation, **6514**(May)
Namabsivayam C, Muniasamy N, Gayatri K, Rani M, Ranganathan K (1996) Removal of dyes from aqueous solutions by cellulosic waste orange peel. Bioressour Technol 57:37–43
Ortiz-Monsalve S, Dornelles J, Poll E, Ramirez-Castrillón M, Valente P, Gutterres M (2017) Biodecolourisation and biodegradation of leather dyes by a native isolate of trametes villosa. Process Saf Environ Prot 109:437–451
Pagilla KR, Canter LW (1999) Laboratory studies on remediation of chromium-contaminated soils. J Environ Eng 125(3):243–248
Panda GC, Das SK, Guha AK (2009) Jute stick powder as a potential biomass for the removal of congo red and rhodamine B from their aqueous solution. J Hazard Mater 164(1):374–379
Pathania D, Sharma A, Siddiqi ZM (2016) Removal of congo red dye from aqueous system using Phoenix dactylifera seeds. J Mole Liquids 219:359–367. https://doi.org/10.1016/j.molliq.2016.03.020
Peng SH, Wang R, Yang LZ, He L, He X, Liu X (2018) Biosorption of copper, zinc, cadmium and chromium ions from aqueous solution by natural foxtail millet shell. Ecotoxicol Environ Saf 165:61–69
Qu J, Zang T, Gu H, Li K, Hu Y, Ren G, Xu X, Jin Y (2015) Biosorption of Copper Ions from Aqueous Solution by Flammulina velutipes Spent Substrate. Bioressources.com 10(4):8058–8075
Rai MK, Shahi G, Meena V, Meena R, Chakraborty S, Singh RS, Rai BN (2016) Removal of hexavalent chromium Cr (VI) using activated carbon prepared from mango kernel activated with H3PO4. Resour-Efficient Technol, **2**, S63–S70. [online] http://linkinghub.elsevier.com/retrieve/pii/S2405653716300707
Ramírez G, Recio FJ, Herrasti P, Ponce-de-León C, Sirés I (2016) Effect of RVC porosity on the performance of PbO2 composite coatings with titanate nanotubes for the electrochemical oxidation of azo dyes. Electrochim Acta 204:9–17
Rangabhashiyam S, Balasubramanian SSP (2018) Assessment of hexavalent chromium biosorption using biodiesel extracted seeds of Jatropha sp. Ricinus sp. and Pongamia sp. Int J Environ Sci Technol. https://doi.org/10.1007/s13762-018-1951-0
Rangabhashiyam S, Selvaraju N (2015) Adsorptive remediation of hexavalent chromium from synthetic wastewater by a natural and ZnCl2activated Sterculia guttata shell. J Mol Liq 207:39–49

Rasool K, Lee DS (2013) Characteristics, kinetics and thermodynamics of Congo Red biosorption by activated sulfidogenic sludge from an aqueous solution. Int J Environ Sci Technol 12(2):571–580

Rezaei H (2016) Biosorption of chromium by using Spirulina sp. Arabian J Chem 9(6):846–853. https://doi.org/10.1016/j.arabjc.2013.11.008

Schmidt C, Berghahn E, Ilha V, Granada CE (2019) Biodegradation potential of Citrobacter cultures for the removal of amaranth and congo red azo dyes. Int J Environ Sci Technol 16(11):6863–6872. https://doi.org/10.1007/s13762-019-02274-x

Selatnia A, Madani A, Bakhti MZ, Kertous L, Mansouri Y, Yous R (2004) Biosorption of Ni2+ from aqueous solution by a NaOH-treated bacterial dead Streptomyces rimosus biomass. Miner Eng 17:903–911

Selmi T, Seffen M, Celzard A, Fierro V (2020) Effect of the adsorption pH and temperature on the parameters of the Brouers—Sotolongo models.Environ Sci Pollut Res 27:23437–23446

Shaban M, Abukhadra MR, Aslam A, Khan P, Jibali BM (2017) Removal of Congo red, methylene blue and Cr (VI) ions from water using natural serpentine. J Taiwan Instit Chem Eng. https://doi.org/10.1016/j.jtice.2017.10.023

Urano K, Tachikawa H (1991) Process development for removal and recovery of phosphorus from wastewater by a new adsorbent 2 adsorption rates and breakthrough curves. Ind Eng Chem Res 30(8):1897–1899

Wang XS, Chen JP (2009) Biosorption of Congo red from aqueous solution using wheat bran and rice bran: batch studies. Sep Sci Technol 44(6):1452–1466

Wang Q, Guan Y, Liu X, Yang M, Ren X (2012) Micron-sized magnetic polymer microspheres for adsorption and separation of Cr(VI) from aqueous solution. Chinese J Chem Eng 20(1):105–110. https://doi.org/10.1016/S1004-9541(12)60369-3

Wanyonyi WC, Onyari JM, Shiundu PM, Mulaa FJ (2019) Effective biotransformation of reactive black 5 dye using crude protease from Bacillus cereus strain KM201428. Energy Procedia 157:815–824

Weber WJ, Morris J (1963) Kinetics of adsorption on carbon from solution. J Sanit Eng Div 89:31–39

Wekoye JN, Wanyonyi WC, Wangila PT, Tonui MK (2020) Kinetic and equilibrium studies of Congo red dye adsorption on cabbage waste powder. Environ Chem Ecotoxicol 2:24–31

Wu W, Chen D, Li J, Su M, Chen N, Chen N (2018) Enhanced adsorption of uranium by modified red muds: adsorption behavior study. Environ Sci Pollut Res, (Vi)

Yang Y, Wang G, Wang B, Li Z, Jia X, Zhou Q, Zhao Y (2011) Biosorption of Acid Black 172 and Congo Red from aqueous solution by nonviable Penicillium YW 01: kinetic study, equilibrium isotherm and artificial neural network modeling. Bioresour Technol 102(2):828–834. https://doi.org/10.1016/j.biortech.2010.08.125

Yang H-D, Zhao Y-P, Li S-F, Fan X, Wei X-Y, Zong Z-M (2016) Removal of hexavalent chromium from aqueous solution by calcined Zn/Al-LDHs. Water Sci Technol 74(1):229–235

Zbair M, Ainassaari K, Assal ZE, Ojala S, Ouahedy NE, Keiski RL, Bensitel M, Brahmi R (2018) Steam activation of waste biomass: highly microporous carbon, optimization of bisphenol A, and diuron adsorption by response surface methodology. Environ Sci Pollut Res 25:35657–35671

Zhang Z, Moghaddam L, O'Hara IM, Doherty WOS (2011) Congo Red adsorption by ball-milled sugarcane bagasse. Chem Eng J 178:122–128. https://doi.org/10.1016/j.cej.2011.10.024

Zhou M, Ju Z, Yuan D (2018) A new metal–organic framework constructed from cationic nodes and cationic linkers for highly efficient anion exchange. Chem Commun 24:2998–3001

Zhoui X, Korenaga T, Takahashi T, Moriwake T, Shinoda S (1993) A process monitoring/controlling system for the treatment of wastewater containing chromium(VI). Water Res 27(6):1049–1054

Zhu J, Li J, Li Y, Guo J, Yu X, Peng L, Han B, Zhu Y, Zhang Y (2019) Adsorption of phosphate and Photodegradation of cationic dyes with BiOI in phosphate-cationic dye binary system. Sep Purif Technol 223:196–202